

# Flycatcher: Fusion of Gaze with Hierarchical Image Segmentation for Robust Object Detection

by

Jeffrey M. Bartelma

B.S., Massachusetts Institute of Technology (2003)

Submitted to the department of Electrical Engineering and Computer Science in  
Partial Fulfillment of the Requirements for the Degree of

Master of Engineering in Electrical Engineering and Computer Science  
at the

Massachusetts Institute of Technology

July 2004 [September 2004]

© Massachusetts Institute of Technology 2004. All rights reserved.

The author hereby grants to MIT permission to reproduce and distribute publicly  
paper and electronic copies of this thesis document in whole or in part.

Author .....

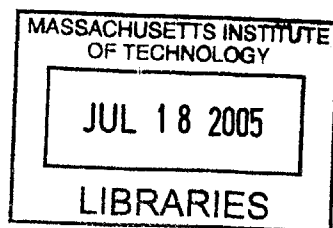
Department of Electrical Engineering and Computer Science  
July 21, 2004

Certified by .....

Deb Roy  
Associate Professor of Media Arts and Sciences  
Thesis Supervisor

Accepted by .....

Arthur C. Smith  
Chairman, Departmental Committee on Graduate Students



**BARKER**

1/1/2020

# Flycatcher: Fusion of Gaze with Hierarchical Image Segmentation for Robust Object Detection

by Jeffrey M. Bartelma

Submitted to the Department of Electrical Engineering and Computer Science  
on July 21, 2004 in partial fulfillment of the requirements for the degree of  
Master of Engineering in Electrical Engineering and Computer Science

**ABSTRACT.** We present Flycatcher, a prototype system illustrating the idea of gaze-based image processing in the context of object segmentation for wearable photography. The prototype includes a wearable eye tracking device that captures real-time eyetraces of a user, and a wearable video camera that captures first-person perspective images of the user's visual environment. The system combines the deliberate eyetraces of the user with hierarchical image segmentation applied to scene images to achieve reliable object segmentation. In evaluations with certain classes of real-world images, fusion of gaze and image segmentation information led to higher object detection accuracy than either signal alone.

Flycatcher may be integrated with assistive communication devices, enabling individuals with severe motor impairments to use eye control to communicate about objects in their environment. The system also represents a promising step toward an eye-driven interface for "copy and paste" visual memory augmentation in wearable computing applications.

Thesis Supervisor: Deb Roy  
Title: Associate Professor of Media Arts and Sciences

# Contents

<b>CHAPTER 1: INTRODUCTION AND MOTIVATIONS .....</b>	<b>6</b>
<b>CHAPTER 2: OBJECT SEGMENTATION USING EYE MOVEMENTS .....</b>	<b>10</b>
2.1 Gaze-Based Input and Control.....	10
2.2 An Eyetrace Interface .....	12
2.3 Experiments .....	14
2.3.1 Equipment .....	14
2.3.2 Procedure.....	15
2.3.3 Stimuli .....	17
2.4 Object Segmentation Using Eye Movements.....	19
2.4.1 Algorithm.....	20
2.4.2 Establishing Ground Truth by Manual Image Annotation .....	21
2.4.3 Results .....	22
<b>CHAPTER 3: OBJECT SEGMENTATION USING COMPUTER VISION .....</b>	<b>25</b>
3.1 Hierarchical Image Segmentation .....	25
3.2 Evaluation .....	26
<b>CHAPTER 4: OBJECT SEGMENTATION BY COMBINING EYE MOVEMENTS AND COMPUTER VISION .....</b>	<b>28</b>
4.1 The Fusion Method.....	28
4.2 Algorithm.....	29
4.3 Algorithm Rationale.....	31
4.4 Example .....	34
4.5 Results .....	34
<b>CHAPTER 5: CONTRIBUTIONS.....</b>	<b>39</b>
<b>REFERENCES .....</b>	<b>40</b>
<b>APPENDIX A: SUBJECT INSTRUCTIONS FOR EXPERIMENTS.....</b>	<b>41</b>

## **Acknowledgments**

The author gratefully acknowledges Yair Ghitza for providing an implementation and description of the Kropatsch and Haxhimusa hierarchical segmentation algorithm, as well as Deb Roy, Josh Juster, and Aditi Garg for helpful comments and suggestions.

## Chapter 1: Introduction and Motivations

Continued innovation in hardware design is making it increasingly practical to move computation away from the desktop and into our everyday lives. Driven by demand for products such as portable audio decoders, compact, high-capacity storage devices have recently become fairly inexpensive. At the same time, the burgeoning popularity of camera phones in the U.S., Europe and especially Japan, where market penetration is projected to reach nearly 100% in 2005[1], demonstrates a mass interest in high-availability autobiographical image capture. This confluence of factors makes it practical and timely to consider always-available systems for recording a "visual diary" of a person's lifetime experiences, from their point of view[2].

In this paper we describe an interface to an image capture system that integrates the user's eye gaze, captured using a wearable eye tracker, to help determine which region of an image is of particular importance to the user. In essence this is the classic problem of object segmentation expressed in the context of a human-assistive system. This is an important problem for several reasons. First, to the extent that major ingredients of a solution are not particular to object segmentation it will provide an initial model for how to simplify traditionally difficult image processing problems using gaze information. Second, the determination of meaningful, salient, or otherwise important image areas would provide effective means for automatic summarization, indexing and search of captured content. Third, images from portable capture devices are increasingly being used for the direct communication of ideas in a visual form.<sup>1</sup> Identifying the important

---

<sup>1</sup> See <http://picturephoning.com/archives/002604.htm> for a number of examples reported

part of an image amounts to enabling the expressive power of indexicals--indicative or demonstrative words such as "this", "that", "these" and "those"--for visual communication.

This final point is a significant one and underlies a key application motivating this work. Over two million individuals with speech impairments in the U.S. alone[3] rely on Augmentative and Alternative Communication (AAC) devices to help express their everyday thoughts, needs, and ideas. Some of these devices now support extensible symbolic vocabularies, from which a user can assemble utterances for visual or spoken output. However, the means of extension are too cumbersome to permit new symbols to be defined on demand, for immediate use in an utterance. On the timescale of a conversation, this shortcoming limits AAC users to relatively small, fixed vocabulary which acts to isolate them from their present environment and conversational partners. For the sake of concreteness let us consider a specific scenario illustrating the problem:

An AAC user, Allen, and his mother go to a department store to find him clothes for a wedding in the family. Allen's mother finds six different ties and eight different sports jackets, and asks for his opinions. Allen's AAC device might contain symbols for sports jackets and ties, but it doesn't have a way to refer to a specific tie, nor a specific sports jacket or any of its parts.

Allen thinks one of the blue ties is too narrow, and dislikes the large buttons on one of the jackets. In a similar situation, most people would point at the narrow tie and say, "That is too narrow", and similarly for the jacket, "Those buttons are too big".

Unfortunately Allen has no effective means of pointing, either physically or

---

in recent print media.

grammatically (with demonstrative words like this, that or those). Using his present AAC device it may be too difficult or time consuming for Allen to say anything more than "The tie on left; the jacket on right". Without access to indexicals Allen is unable to speak effectively about his immediate spatiotemporal surroundings.

Our prototype addresses this problem by enabling a user to capture important parts of a scene using his or her eyes. In this respect the prototype enables a kind of eye-driven "copy-and-paste" operation for copying pieces of the user's environment into his or her electronic communication aid. To capture a cropped image of the sports jacket he wishes to discuss, Allen needs only trace an outline of the jacket with his eyes, pressing a button once to begin his trace, and again to end it. The new symbol could then be used in conversation, that is, displayed to his mother on the device's output screen, and optionally pronounced with a default vocalization of "this" or "that". Preliminary experiments suggest that Flycatcher, our prototype gaze-based object segmenter, substantially solves this example problem for a set of stimuli depicting real-life retail displays including jackets, shirts, pants, and so forth. In this paper we describe how Flycatcher works, focusing particularly on the three core algorithms that together comprise the bulk of its technical contribution:

- processing inherently noisy outlines of an object as traced with the eyes into a reasonable approximation of that object's bounds;
- using the unreliable results of image-based hierarchical segmentation to reinforce one another;
- combining top-down information about the user's intent (derived from eyetraces) with bottom-up information about the structure of the image (derived from



hierarchical segmentation techniques) into a single, more accurate approximation of the region of interest.

The remainder of this paper is structured as follows. Chapter 2 provides background on some relevant aspects of eye gaze analysis and introduces an object segmentation algorithm that uses only gaze information, ignoring the structure of the image itself. We evaluate the performance of the gaze-only algorithm on a set of three experiments. Chapter 3 reviews a purely image-based approach to object segmentation and gives an informal evaluation of its performance on the same three datasets. Finally, Chapter 4 presents and evaluates a new algorithm that incorporates gaze information into a hierarchical segmentation technique to achieve more robust object segmentation.

## Chapter 2: Object Segmentation Using Eye Movements

### 2.1 Gaze-Based Input and Control

As we discuss more fully in the next section, image-based object segmentation is an extremely difficult problem that has largely eluded computer vision researchers for decades.<sup>2</sup> In assistive systems designed to aid or enhance the capabilities of a human user, under some circumstances it makes sense for the human to assist *the system* in solving some subproblem that is easy for people and hard for computers, provided it is possible to do so in an unobtrusive way. Image-based object segmentation and object recognition are just two problems where a small human investment in effort can pay very large dividends in the overall usefulness of the integrated system. In the case of icon capture for AAC devices, there is a profound difference of utility between a fully automatic object segmenter that does not work and a mostly automatic object segmenter that does.

There are obvious advantages to using gaze information to control a computer system. This is especially true of systems intended to aid non-verbal or other disabled populations, because many individuals with partial paralysis or poor limb dexterity nonetheless can control their eyes. In such cases gaze input may be one of the only options[5]. More generally, gaze control leaves the hands free or mostly free, which is of course crucial for always-on applications. Even when hands-free operation is not

---

<sup>2</sup> If we accept that humans' ability to parse unfamiliar scenes into coherent objects is owed in part to domain knowledge accumulated from a lifetime of interaction with the world, it is also an underdetermined problem. Practical systems incorporating an object segmentation component often define their own models of what constitutes an object, according to the needs of the system and the environment in which it operates[4].

important there is evidence that gaze-based selection is faster than using a conventional selection device such as a mouse, at least in some circumstances[6].

However there are a number of important caveats and potential pitfalls associated with eye control. First, most present eyetracking systems are still expensive and bulky, and not very practical particularly for mobile use. However there are some encouraging trends in this regard. Some models of Canon cameras are now equipped with eye-controlled autofocus systems[7], and IBM's BlueEyes research project is exploring the value of eye-tracking, among other input modalities, in producing more user-aware consumer electronics[8].

A more lasting issue affecting gaze-based control is that what we believe our eyes to be doing and what they are really doing are rarely the same thing. For example, when we perceive our eyes to be motionlessly fixating on a stationary object, they are actually in constant involuntary motion, and occasionally make large saccades of 15-20 degrees of visual angle with neither our knowledge nor control[9]. Similarly, what we believe to be smooth, uninterrupted tracking of figures is in fact a set of discrete stops and small (involuntary) saccades, not always even lying on the line one is trying to track[9]. And although we perceive that we can move our eyes either quickly or slowly, individual saccades are themselves limited in amplitude to 20 degrees and of fixed duration given an amplitude. In other words, not only are voluntary eye movements subject to limited conscious control, but we are not even normally aware of this fact. Finally, eyes move very quickly--peak angular velocity is about 1 degree per millisecond--so appropriately recording eye movements requires equipment accurate on a very fine timescale.

Apart from these difficulties inherent to nature of eye movements, eyetracking systems are also susceptible to several kinds of measurement error. Yarbus' original experiments were performed using an invasive technique involving eyeball suction clamps and eyelid restraints. Modern techniques, while noninvasive, are prone to several types of error Yarbus did not face (depending on the exact system used):

- imperfect calibration, leading to small, mostly translational inaccuracies;
- horizontal and vertical correlation factors calculated by the calibration process that may not be accurate for all regions of an image, therefore causing distortion of the trajectory trace, especially near the extremes of an image;
- temporary loss of infrared corneal reflection (usually due to blinks) needed to calculate where the user is looking causing erratic leaps and spikes in eyetraces.

The accuracy of recorded data also depends to some extent on the nature of the control interface. If the interface requires unnatural movements such as long fixations or intentional blinking, the resulting eyestrain will decrease accuracy by introducing extra noise. But even with a natural control interface, if we are to use gaze information as input for an object segmenter, we must be prepared to clean up inherently noisy data.

## **2.2 An Eyetrace Interface**

There are many possible gaze-based interfaces for incorporating users' knowledge of object boundaries into the classic problem of object segmentation. For example, one could ask users to denote interesting regions by:

- pressing a button while looking at the center of the region;
- pressing a button while looking at each of several locations within the region of

interest, to mark them all as part of the same object;

- or, looking at and marking with button presses the top, bottom, leftmost and rightmost points of the region of interest.

Our prototype system, Flycatcher, instead asks users to create *eyetraces*, that is, to trace a rough outline of the region of interest with their eyes, pressing a button to indicate the beginning and end of the tracing process. There are several advantages to this choice. First, it is a fairly intuitive way to mark part of an image as interesting or important, similar, for example, to how we circle a location on a map. Second, it is possible to derive from the eyetrace at least approximations to the same data we could collect directly through a less intuitive interface. For example, our methods use the eyetrace to approximate the centroid of the region as well as a number of points interior to it. Finally, and crucially, the eyetrace provides a strong hint as to the approximate overall size of the region to be captured. As we will more fully explain in Section 4, this allows Flycatcher to choose which of several candidate regions hypothesized by analyzing the image itself is most likely the best answer.

Flycatcher uses keypresses to signify that the system should begin and end the recording of an eyetrace. However our framework is general, and keypresses could be trivially replaced by another input modality, e.g. simple vocalizations. Additionally it may be possible to further streamline the interface to require only one such signal by intelligently closing partial eyetraces, but our early prototype does not attempt this.

Using the gaze interface outlined above we collected eyetracking data from subjects for three experiments. The data from these experiments were used to evaluate the efficacy of our object segmentation algorithms. We now describe our experimental

methodology.

## **2.3 Experiments**

### **2.3.1 Equipment**

In the experiments, subjects (MIT graduate and undergraduate students) used a wearable eyetracker (I-Scan Model ETL-500) which includes two miniature video cameras mounted on a headband. The first camera, the eye camera, is directed towards the user's left eye. Using infrared illumination, it provides reliable video of the subject's eye movements which are converted into point-of-regard (POR) information by I-Scan's image processing firmware. A second scene camera is also mounted on the headband. It points outwards to capture a view of the environment as seen from the subject's perspective. Although the current configuration of hardware (head worn eye tracker tethered to a workstation) is not immediately suitable for mobile wearable operation, we envision future versions of the hardware in which the eye and scene camera are further miniaturized and integrated into a wearable device resembling a pair of ordinary eye glasses.[2]

The eyetracker generates the  $x$ - $y$  coordinates of the subject's visual point of focus at a rate of 60 samples per second and sends them to the serial port of a data recording computer along with video from the scene camera. Frames are received at a rate of 15-20 frames per second at a resolution of 320 x 240 pixels.

The video and point-of-regard data is recorded using a custom program which maintains a buffer of the last 10-15 seconds of timestamped frames and their corresponding PORs. When a key is pressed to signify the beginning of an eyetrace, the

current timestamp  $t1$  is noted. When a keypress arrives at  $t2$  to signify the end of an eyetrace, all frames between  $t1$  and  $t2$  are retrieved from the buffer and saved to disk for future processing. If eye motion is slow at some point during the recording, adjacent frames will bear the same POR information. Such duplicate frames are not saved as they contain no new information.

This "buffer-and-fetch" architecture is a necessary consequence of the extreme time sensitivity of eye movements. If significant processing—for example, special setup to store frames—is triggered at  $t1$ , the regularity of reading and buffering subsequent frames is disrupted, and the resulting eyetrace data is inaccurate. By delaying all processing until after  $t2$ , only the frames read after  $t2$  (which we do not care about) are affected.

### **2.3.2 Procedure**

The three experiments were almost identical aside from the stimuli used. Subjects were seated approximately 10 feet away from a stimulus array situated on a empty white wall.

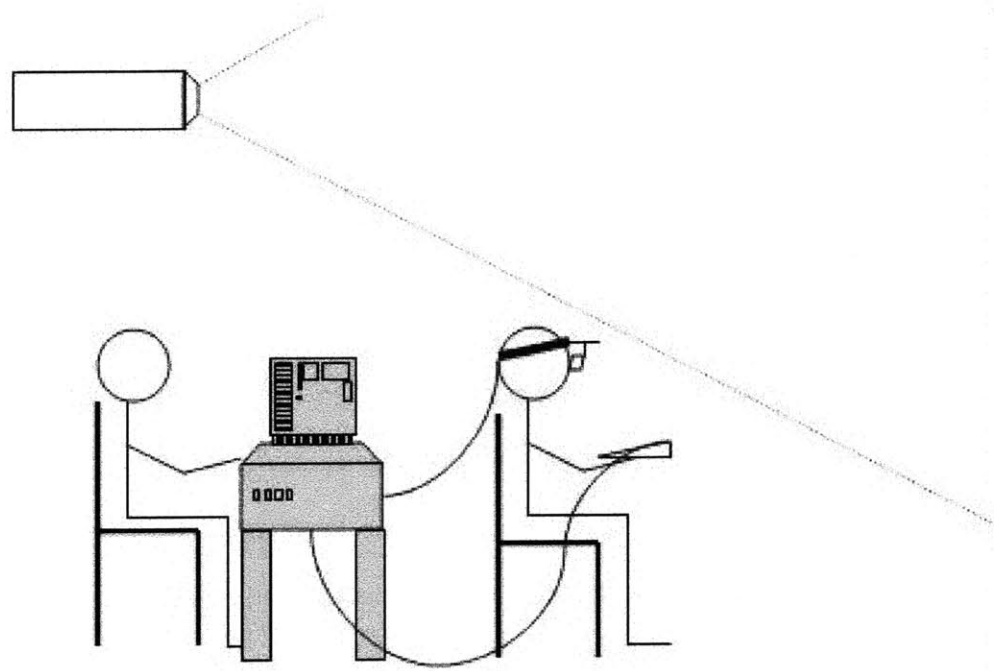


**Figure 1.** Experimental setup. An experimenter (left) controlled an overhead LCD projector displaying stimuli on a wall in front of the subject.

See Figure 1. In each of 15-25 trials an experimenter read the subject a short description of one of the stimuli visible on the wall, for example, "the blue triangle". Subjects were instructed to outline the stimulus with their gaze (i.e. trace its outermost contour), using the space bar of a keyboard to signify the beginning and end of the outlining process. Subjects typically rested their hands on the keyboard and so did not need to look away from the stimulus to find the space bar. Subjects were instructed to trace at a speed they found personally comfortable. Following the subject's second button press, the experimenter paused several seconds before describing another stimulus for the next trial. See Appendix A for the full text of instructions given to subjects.



### 2.3.3 Stimuli

Although subjects faced the same tasks in all three experiments, the stimuli for each experiment were different and were chosen for different reasons.

The purpose of Experiment 1 was to act as an initial, simplified proving ground for our gaze-based segmentation algorithms. The stimuli for Experiment 1 are five shapes cut out of colored construction paper: a red rectangle, a blue triangle, a maroon semicircle, a black square, and a green "peanut" shape.

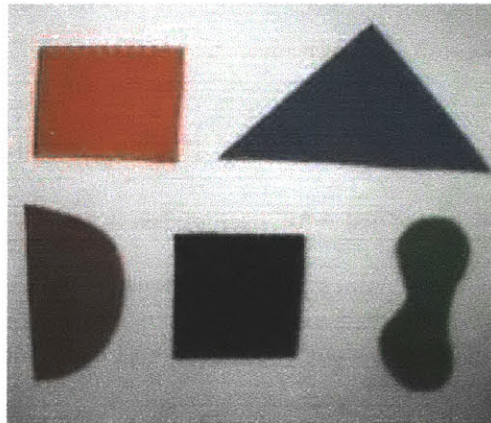


**Figure 2.** Stimulus array for Experiment 1.

See Figure 2. These stimuli served as a valuable testbed, with unambiguous correct and incorrect answers, for developing techniques combining gaze and image-based information. Furthermore the sharp edges of these stimuli helped us to a clearer picture of the noise contained in real-life eyetracking data, as there could be no doubt which contours subjects were trying to trace. We recorded data from three subjects for this pilot experiment.

The purpose of Experiment 2 was to test the performance of the prototype on one of the actual motivating problems for this thesis. The stimuli for this experiment are color digital photographs of real-life retail displays in Cambridge, MA stores taking during

daylight hours.



**Figure 3.** Representative stimuli for Experiment 2.

See Figure 3 for some representative examples. The stimuli realistically simulate scenarios in which a speech-disabled AAC user wishes to capture an image of some item, for example, a specific jacket or pair of pants, in order to talk about it. The photographs were projected on the wall of a darkened room from an LCD projector situated behind the subject as shown in Figure 1. As in Experiment 1, the experimenter read descriptions of target objects (e.g., “the blue jacket in the middle”) to prompt participants to trace objects. We recorded data from 4 subjects for this experiment.

The purpose of Experiment 3 was to test the performance of the prototype segmenting objects from natural scenes. The dataset was chosen to shed some light on modes of failure for images with complex color and illumination makeup. The stimuli for this experiment are 26 color digital photographs selected from the Berkeley Segmentation Dataset and Benchmark[10]. The photographs include animals in the wild, flowers, boats, people, statues, and so forth.

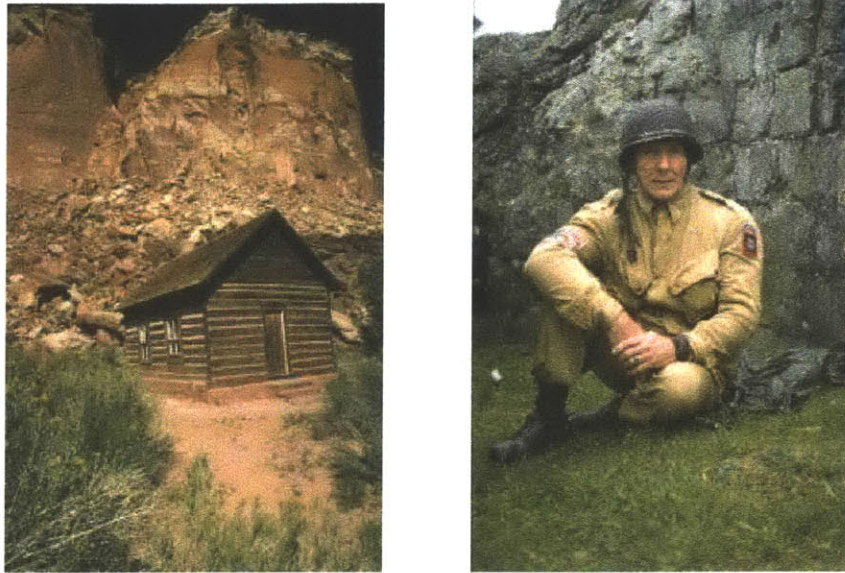


**Figure 4.** Representative stimuli for Experiment 3.

See Figure 4 for representative examples. As in Experiment 2, stimuli were displayed using an overhead LCD projector to a total of four subjects. For Experiment 3 subjects were given the additional instruction that if an object had a very complex shape, it would be acceptable to simplify the outline, and that they should do whatever they found most comfortable. For example, rather than tracing the legs of a horse individually, subjects could simply sweep their gaze under all four hooves at once. For the most part subjects did choose to simplify complex outlines. Aside from the stimuli used this was the only difference between the three experiments.

## **2.4 Object Segmentation Using Eye Movements**

We will begin our exploration of gaze-based object segmentation by discussing algorithms that take into account only the gaze information we collected, and ignore information in the image itself.

The raw eyetraces collected from users in Experiments 1, 2, and 3 include many of the previously described errors common to noninvasive eyetracking. Imperfect calibration is evident in the form of small translational inaccuracies. Eyetraces are sometimes distorted at the top and bottom extremes of images and are frequently interrupted by a blink, which is then followed by random noise. We also found that subjects purporting to trace the contours of an object often actually "cut corners" or exclude the edges of the area. Anecdotally, the faster a subject completed his or her eyetraces, the more likely they were to have cut corners. Most eyetraces were completed in 2-3 seconds; slightly longer times were typical for complex outlines (wildlife), and shorter times for very simple ones (an oval).

Due to the noise observed, the rectangular bounds of the eyetrace itself are often poor indicators of the true spatial extent of the traced object. To generate a better approximation of the region of interest represented by an eyetrace, we have developed the following algorithm. Given a raw eyetrace in the form of a sequence of video frames from the eyetracker scene camera and their respective PORs, the algorithm produces a rectangular bounding box representing the hypothesized region of interest.

#### **2.4.1 Algorithm**

1. Filter the sequence of frames to remove all those recorded during or after a blink, as these frames typically contain only erratic, misleading noise. (With the ISCAN ETL-500, blinks typically appear as sudden jumps of the POR to  $(0,0)$ ).
2. Interpret the PORs for remaining frames to define a (possibly self-intersecting)

polygon  $P$ .

3. Beginning with the smallest rectangle  $R$  that bounds  $P$ , iteratively “slide in” (by  $STEP\_SIZE$  pixels) the side of  $R$  which would result in a new rectangle excluding the smallest possible area of  $P$ . Continue until  $R$  bounds only  $FRACTION$  percent of  $P$ 's total area.
4. Grow the resulting rectangle in accordance with its present aspect ratio until it contains the POR for the first frame in the sequence.
5. Add a small pad of minimum thickness  $PAD$  pixels to the perimeter of the rectangle, again in accordance with its present aspect ratio.

Our present implementation uses  $FRACTION=0.85$ ,  $STEP\_SIZE=1$ , and  $PAD=4$ . However any similar numbers also work without significantly damaging performance.

The rationale for this bounding box “squashing” operation is as follows. Both our limited conscious eye control and inherent measurement error set practical limits on the precision of recorded eyetraces. For this reason most very sharp spikes are apt to represent meaningless noise rather than an intentionally drawn object boundary. In the sense that this algorithm penalizes long thin protrusions it can be likened somewhat to a crude low-pass filter. The growing operation of step 4 arises from the observation that subjects frequently begin their eyetrace with gaze fixed exactly on the target contour, even if they diverged significantly later. Lastly step 5 attempts to reclaim the small amount of legitimate object area that may have been excluded during the previous squash operation, as well as compensate for many users’ tendency to “cut corners” or exclude a region’s edges when tracing it.

#### **2.4.2 Establishing Ground Truth by Manual Image Annotation**

To facilitate a quantitative analysis of the results, an experimenter hand-marked every test image with a rectangular bounding box  $G$  (the *ground truth*, or official solution) tightly bounding the object the subject was asked to trace. Annotation was performed using a lightweight piece of custom software. The software enables an annotator to draw a box superimposed on the scene camera image using an ordinary mouse with a crosshair cursor.

### 2.4.3 Results

We assessed the overall quality of the algorithm's output rectangle  $R$  using the measure

$$q = \frac{|G \cap R|}{|G \cup R|}$$

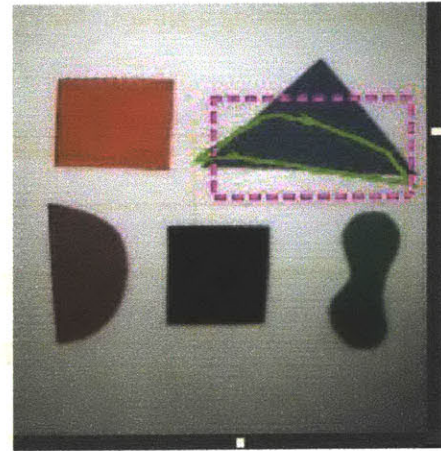
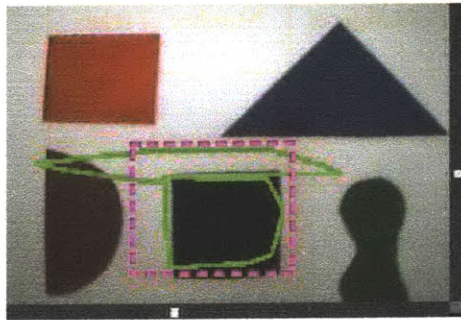
a ratio of the number of pixels enclosed in both rectangles to the total number of pixels enclosed in at least one of the rectangles. Note the formula penalizes both *misses*—pixels contained in the actual solution  $G$  but not the hypothesized solution  $R$ —and *false alarms*—pixels contained in  $R$  but not  $G$ . In so doing this measure encompasses all major factors by which two rectangles can be said to differ:  $x$  position,  $y$  position, aspect ratio, total area, and so forth. The measure reaches its maximum of 1.0 only when the ground truth and proposed solution are identical. It considers all proposed solutions that do not overlap the ground truth at all ( $q=0.0$ ) to be equivalently, and maximally, unsuitable approximations. This behavior corresponds to the reasonable intuition that all proposed solutions containing zero percent of the desired area are equally worthless. Additionally the measure has the desirable properties of numeric stability (so it can be

meaningfully averaged, multiplied, etc.) and symmetry (allowing more efficient pairwise comparisons among a group). The results are shown in Table 1:

Experiment no.	Median quality $q$	Number of subjects	Number of trials
1	0.59	3	69
2	0.66	4	82
3	0.66	4	111

Table 1. Gaze-only results.

As can be seen from the table performance remains stable as image complexity increases and is just as good for natural images as the intentionally simplified problem. When combining eyetracking information with information in the image itself (as we will describe in Section 4) the purely gaze-based algorithm represents a reasonable fallback solution for complex images where bottom-up object segmentation techniques provide little useful information. Figure 5 shows some results of this algorithm on stimuli from the first two experiments.



**Figures 5a and 5b.** Sample gaze-only results for Experiment 1. The eyetrace is shown in green; the hypothesized region of interest is shown as a dashed magenta box. Figure 5a (left) shows how the “box squashing” algorithm ameliorates the effects of noise spikes in the eyetrace. Figure 5b demonstrates that when the eyetrace is poor—here the subject has “short-cut” the top vertex of the triangle—the gaze-only algorithm can pay dearly for ignoring boundaries in the image itself.



**Figures 5c and 5d.** Sample gaze-only results for Experiment 2. Figure 5c illustrates the often-large performance gain achieved by simple noise filtering. Figure 5d shows that with no knowledge of the underlying image the gaze-only algorithm cannot recover from problems such as translational calibration error.



## Chapter 3: Object Segmentation Using Computer Vision

Generic object segmentation, i.e., parsing an arbitrary image into regions corresponding to human judgments of object boundaries, is an unsolved problem of computer vision.

The lesser problem of robustly dividing an image into coherent regions based on color is also surprisingly elusive. Although there are many approaches to this latter problem[11] in general they are unreliable. Here we explore the behavior of one recent color-based segmentation algorithm on our three data sets.

### 3.1 Hierarchical Image Segmentation

Kropatsch and Haxhimusa's hierarchical segmentation algorithm[12] produces from an image and a seed point  $P$  a set of hierarchically related regions of points which contain  $P$ . In other words, each region in the set contains all regions smaller than itself.

The algorithm proceeds in two main stages. The first stage performs connected component analysis based on Saturation and Value channels in HSV space (Hue, Saturation, Value). Hue is ignored due to image properties of the scene camera. For every pixel in the image, the two-channel values are stored in a color map structure. The color map is then scanned to find ten representative colors. The representative colors are added incrementally and are chosen based on maximum distance from each previously found representative color. Each pixel is then set to its nearest representative color, based on its original color and proximity in SV space. Finally, connected component analysis is performed to group locally adjacent regions of the same color.

The second stage of the algorithm performs graph contraction of the previously found connected components. Each component is treated as a node in a graph, with edges

connecting adjacent regions in the graph. For a specified number of iterations, locally adjacent nodes are grouped based on distance in SV color space. Grouped nodes are then contracted to form one node while preserving the adjacency structure of the graph. This iterative approach allows for multiple “levels” of segmentation and accounts for the hierarchical nature of the results: each iteration of graph contraction potentially grows the region containing  $P$ .

If we consider the seed point  $P$  to represent the current focus of a user's gaze, we can interpret the set of regions produced by the algorithm as hypotheses regarding the spatial extent of likely objects containing  $P$ . For example, if the user's point of regard were resting on a coffee cup atop a table, segmentation level 2 might be the region of points comprising the cup, and segmentation level 4, produced by two further iterations of graph contraction, might be the region of points comprising the tabletop.

### **3.2 Evaluation**

Using the same three datasets as in the previous chapter, we performed an informal evaluation. Looking ahead to the way eyetraces are employed in our combination method (described in Section 4), to choose a seed point for running the algorithm on each frame, we first calculated the centroid  $C$  of the eyetrace polygon and chose a random point  $M$  on eyetrace polygon itself. We then used as a seed the point  $1/3$  the distance from  $C$  to  $M$ . As expected the algorithm performed well on for the colored construction paper blobs of dataset 1. However given the more realistic datasets of Experiments 2 and 3 viewed through the eyetracker's scene camera, performance was quite erratic. The algorithm produces only connected regions, but these regions are typically irregular in

shape and often sprawled across regions of the image containing unrelated parts of the scene. Additionally small translations of the seed point can dramatically change the results.

These issues notwithstanding, strong agreement between adjacent segmentation levels and nearby seed points is often evident. And though the irregular regions themselves seldom correspond to human intuition, often the bounding box of at least one hypothesized region does. That the results, broadly taken, still contain obvious structure despite being generally poor and individually unreliable raises the idea of using cross-hierarchical agreement to help distinguish stable regions from noise. If a particular hypothesis is generated by multiple nearby seed points it is likely to specify a genuine region.

Even so, problems remain: first, if several hypotheses recur in the respective hierarchies of nearby points, the algorithm offers no principled way to choose among them. Second, at the highest level of segmentation (after many graph contractions) the hypothesis generated will be the same almost regardless of seed point; namely, it will be the region containing every point in the image. To figure out the extent of the region that is important to the user, we don't just need cross-hierarchical agreement—we need cross-hierarchical agreement *on a good hypothesis*.

## Chapter 4: Object Segmentation By Combining Eye Movements and Computer Vision

### 4.1 The Fusion Method

We have discussed two very different algorithms for inferring the spatial extent of a particular object in an image. Each of these approaches has both significant strengths and substantial shortcomings. Object segmentation via eyetraces alone provides a clear picture of user intent and generally good performance even for very complex images, but can be derailed by correlation factor errors, calibration problems, accidental overshoot, and other phenomena. Hierarchical image segmentation can exploit color information in the image itself to produce a set of hypotheses regarding the location of objects possibly containing a given point. But it provides no principled way to choose among these hypotheses, which are themselves inherently unstable and non-robust with respect to real-world data.

We have developed a technique which we call the *fusion method* which combines top-down information about the user's intent (derived from eyetraces) with bottom-up information about the structure of the image itself (derived using the hierarchical segmentation algorithm.) When the source images contain visual structure sufficient for hierarchical segmentation to offer at least some good hypotheses, the fusion method provides a principled way to choose among them, and usually performs much better than either method independently. When hierarchical segmentation generates no agreed-upon hypotheses consistent with the gaze data, the fusion method falls back to the gaze-only solution.

The fusion method runs hierarchical segmentation multiple times beginning at a number of seed points derived from the eyetrace. Then it performs similarity-based grouping among the results to obtain a list of self-similar hypothesis groups. Finally, it calculates a prototypical (average) bounding box for each group, and selects as its answer the prototypical box most similar to the gaze-only solution computed as in Section 2, provided it passes a minimum similarity threshold. A detailed description of the algorithm follows.

## 4.2 Algorithm

1. Filter the sequence of frames to remove all those recorded during or after a blink.
2. Calculate the gaze-only solution for the eyetrace as in Section 2. This is the *query box*.
3. Calculate the centroid  $C$  of the eyetrace polygon.
4. Choose a subset of the frames on which to run the hierarchical segmentation algorithm. Our present implementation uses ten evenly spaced frames (the first and the last of the sequence, plus eight frames between, spaced as evenly as possible), but results are fairly insensitive to this number.
5. For each of the frames to be segmented, choose a seed point part way down the line connecting  $C$  and the point of regard for that frame. The present implementation chooses seed points  $1/3$  of the way from  $C$  to the point of regard.
6. Apply a mild Gaussian blur to the frames that will be segmented. This is purely to help the segmenter overlook small noise in the image. The present implementation applies a 5-pixel Gaussian blur. Blur size is not critical.
7. Apply the hierarchical segmentation algorithm to the chosen frames using the calculated seed points.

8. Collect a single master list of hypotheses (each a list consisting of all points in the hypothesized region) generated by the algorithm. For example, if segmenting each of 10 frames to segmentation levels 1, 2, 3, 4, and 5, this list of candidate hypotheses will be 10 \* 5 = 50 elements long.

9. Divide the horizontal and vertical pixel range into NBUCKETS total rectangular buckets. Create a length NBUCKETS vector  $\mathbf{v}$  for each region, setting  $v_i$  to the number of points of that region contained within bucket  $i$ . Finally, for each unique pair of regions compute and store the chi-square divergence

$$D_{x^2}(\mathbf{h}, \mathbf{k}) = \sum_{i \in k_i \neq 0} \frac{(\mathbf{h}_i - \mathbf{k}_i)^2}{\mathbf{k}_i}$$

of their respective vectors  $\mathbf{h}$  and  $\mathbf{k}$ . The present implementation, which operates on 320 x 240 pixel eyetracker images, uses 20 buckets in the  $x$ -direction and 20 buckets in the  $y$ -direction, such that NBUCKETS=400 and each bucket is 16 pixels by 12 pixels in size.

10. Use the pairwise similarities previously calculated to divide the hypotheses into non-overlapping groups. The present implementation uses a single-pass clustering algorithm similar to that of Hill[13]. No two hypotheses with chi-square divergence greater than the empirically chosen value of 200 may be placed in the same group. Modest variations in this number do not affect final results much.

11. Compute a prototypical bounding box for each group by averaging the bounding boxes of its hypotheses.

12. Return the prototypical bounding box with highest similarity quotient  $q \geq \text{TOL}$  to the query box that is also not implausibly small (presently, less than 400 total pixels;

results are not very sensitive to this number). If no such bounding box exists, return the query box itself, that is, the gaze-only solution as calculated in step 2. TOL for the present implementation is 0.375.

### **4.3 Algorithm Rationale**

It is an obvious idea to increase the reliability of an unreliable algorithm by running it multiple times and looking for regularities. However without seed points from the same object, multiple runs of the hierarchical segmentation algorithm are not likely to yield any regularities at all. Of course, if we knew which pixels in the image were and were not from the same object, we would already have an object segmenter and thus no need for seed points.

The eyetrace gives us a way out of this quandary: it is a statement of human judgment that all points interior to the eyetrace belong to the same object. Yet, if this statement were free of all noise and error, it would also be the desired object segmenter and we would never need to examine the image itself. In this way the fusion algorithm performs mutual disambiguation with two noisy data sources.

After grouping hypotheses and computing prototypes for each group (steps 8-11 above), we have the results of what is essentially a more robust, self-reinforcing hierarchical segmentation algorithm. Small amounts of noise or a seed point landing outside the region of interest are unlikely to be disastrous to performance. However, without the eyetrace we still have no principled way to choose between alternatives generated by this more robust segmenter. In this context the eyetrace is regarded as a noisy statement of human judgment regarding spatial extent of the region of interest. By eliminating much of the noise from this statement (as in Section 2) and using it to guide

the choice of segmentation results, the fusion method arrives at a region consistent with information from both the human user and the image itself.

The fusion algorithm falls back to the gaze-only solution when no hypotheses of about the right size are found. The TOL parameter, or *winner tolerance*, defines what is meant by “about the right size”. It describes the maximum amount of deviation we are willing to accept between the output of the gaze-only algorithm and the final output of the fusion method. In essence setting  $TOL=0$  means “always use the best image-based solution, no matter how far it strays from the gaze-based solution” and  $TOL=1$  means simply “always use the purely gaze-based solution”. The setting of TOL is a tradeoff. The lower TOL is, the more dramatic the improvement fusion can achieve over the gaze-only algorithm when the image provides helpful information. But a low setting for TOL also means the fusion method can be led further astray by poor segmentation hypotheses. This is the only parameter for which modest changes produce noticeable differences in the fusion method's final results. That said, over all trials, TOL values ranging between 0.375 and 0.6 demonstrated roughly equivalent aggregate performance.



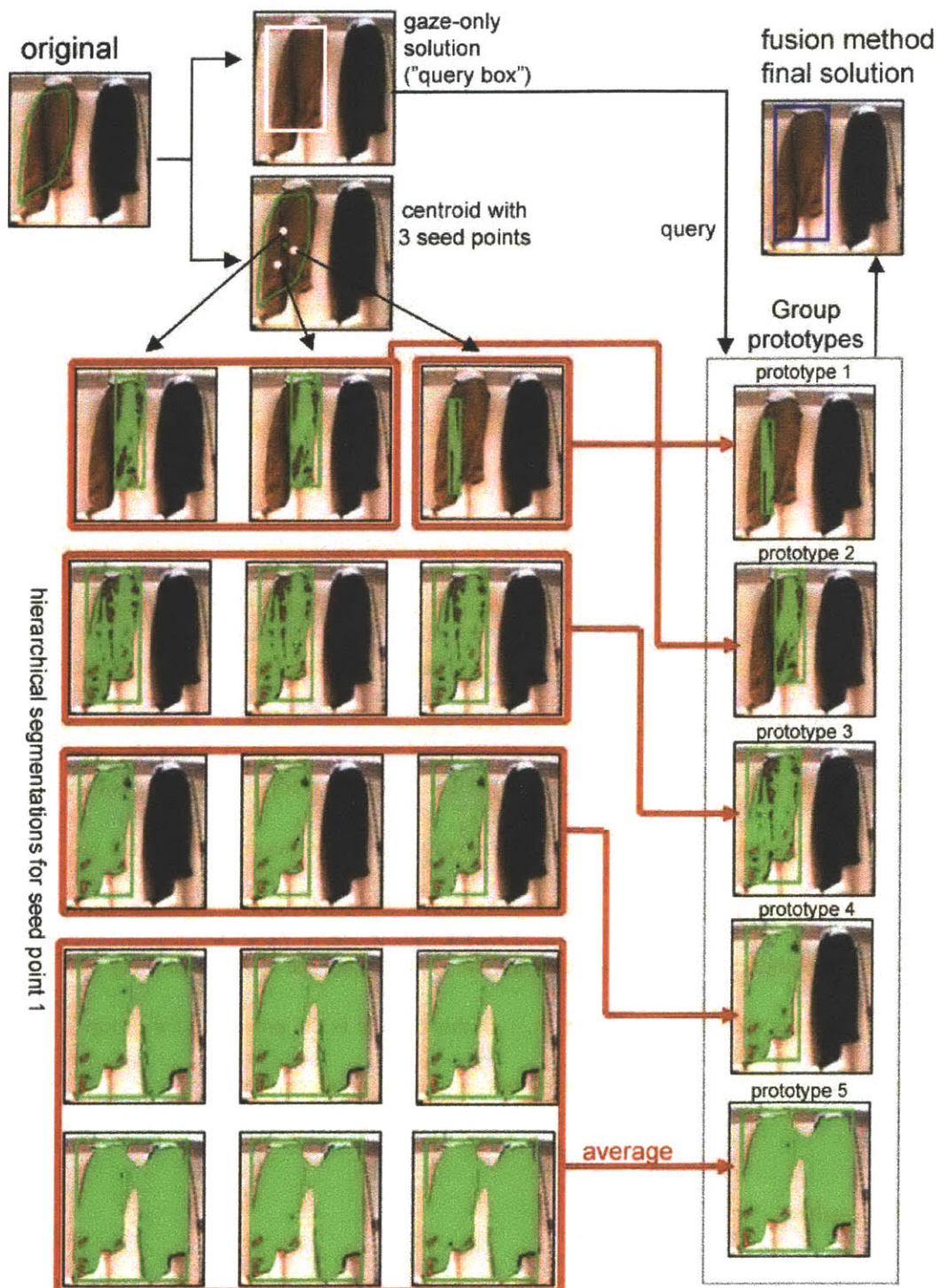


Figure 6. Sample run of the fusion algorithm.

## 4.4 Example

Figure 6 is a pictorial illustration of one complete run of the fusion algorithm. From the original image and its recorded eyetrace we first find the gaze-only solution as in Chapter 2, pictured at top. We then use the eyetrace to calculate seed points for the hierarchical segmentation process. Although the present implementation segments from ten seed points, due to space constraints we only show three, which appear in white.

Each seed point gives rise to a column of segmentation hypotheses, one for each segmentation level. In the figure we show the actual regions hypothesized by segmentation levels 1-5 in bright green. Note that there is significant agreement among hypotheses for both neighboring segmentation levels and neighboring seed points. We divide the 15 total hypotheses into similarity groups to capture the essence of this cross-hierarchical agreement. In this example there happen to be five groups of hypotheses, indicated with red in the diagram. The level 1 segmentation for seed point 3 comprises its own group because it is too dissimilar to every other hypotheses to share in a group. We then calculate a prototype for each group by averaging the bounding boxes of its member hypotheses. Finally, we look for the group prototype whose bounding box most closely matches the gaze-only solution. In this case, it is the prototype for group 3. We return its bounding box as the final solution of the fusion algorithm.

## 4.5 Results

By using gaze-based and image-based analysis techniques to complement one another, the fusion algorithm was able to succeed in many instances where both

techniques separately failed--particularly on dataset 2, the retail displays.

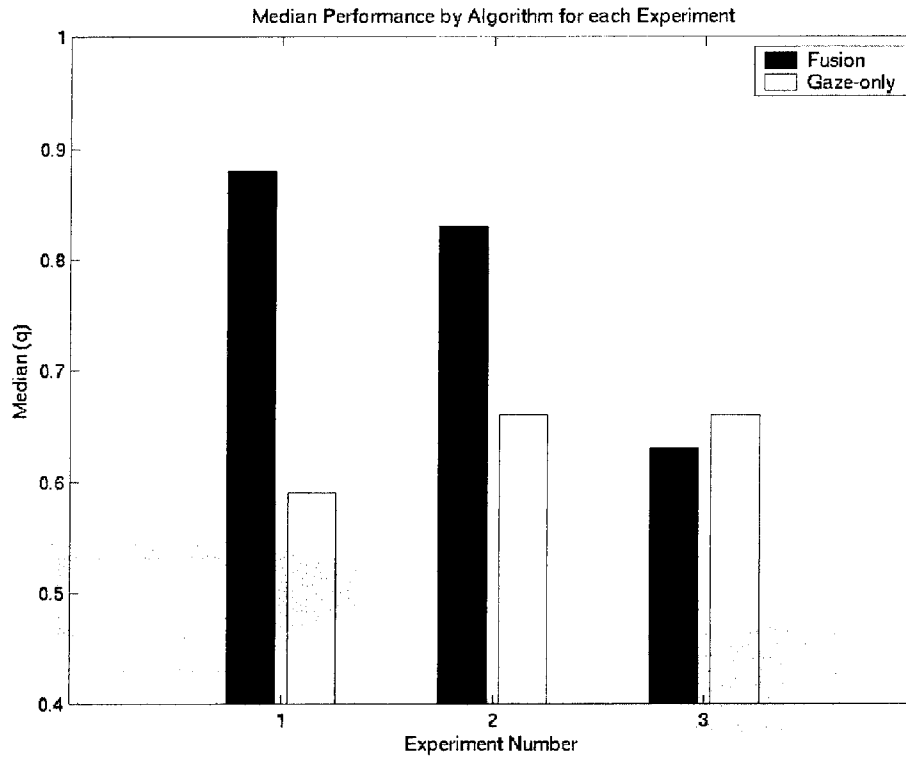
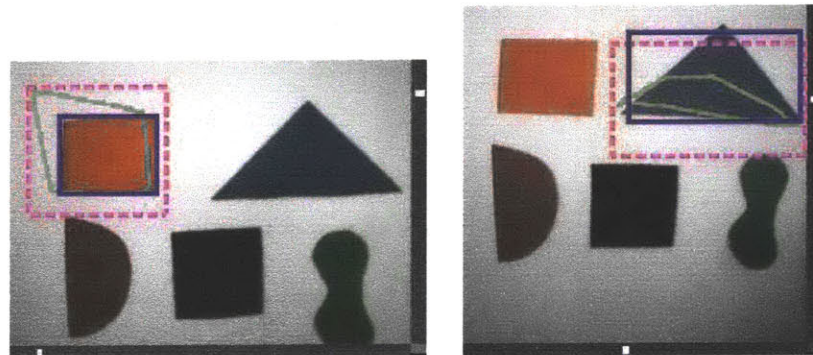


Figure 7. Median performance by algorithm for each experiment.

Experiment no.	Eyetrace $q$	Fusion $q$	Number of subjects	Number of trials
1	0.59	0.88	3	69
2	0.66	0.83	4	82
3	0.66	0.63	4	111

Table 2. Fusion results.

As can be seen<sup>3</sup> from Table 2 the fusion algorithm vastly outperformed the gaze-only algorithm for both datasets 1 and 2. Performance on dataset 1 was exceptionally strong. This was expected because the brightly colored shapes of paper are usually segmented cleanly by Kropatsch and Haxhimusa's original algorithm, thus providing the fusion method with several high-quality hypotheses. Figure 8 shows some typical results. There were few failures; those that did occur were typically caused by a very poor eyetrace which landed the majority of seed points on the wall itself, rather than the colored region.



**Figure 8.** Sample fusion results for Experiment 1. Eyetraces are shown in green, the gaze-only solution is shown as a dashed magenta box, and the output of the fusion algorithm is in blue. Using the color structure of the images the fusion algorithm was able to overcome these inaccurate eyetraces to achieve an excellent solution.

For dataset 3, the gaze-only method had slightly higher median accuracy than the fusion method. Although there were many natural images for which the fusion method bested the gaze-only method--see Figure 9 for some striking examples--there were

---

<sup>3</sup> By way of interpretation it should be noted that achieving a perfect score of 1.0 entails identifying the extent of the desired region down to the very last pixel. In all three datasets, but especially sets 2 and 3, region borders are frequently unclear, and certainly are not sharp to single-pixel accuracy. A score of 0.90 or greater is very good.

slightly more instances in which the underlying segmenter generated misleading hypotheses bounds nonetheless sufficiently similar to the gaze-only results to be accepted as the final output. See Figure 10. Given the typically poor results of the underlying segmenter on such images this too was expected.

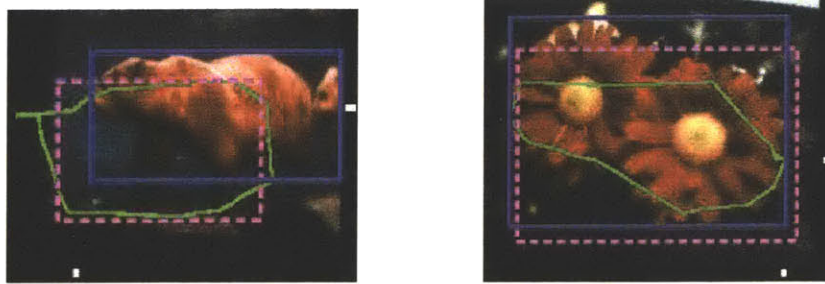


**Figure 9.** In these two natural images from Experiment 3 the hierarchical segmenter discovered enough color structure to successfully override a translational calibration inaccuracy (left) and a relatively imprecise eyetrace (right).



**Figure 10.** Interesting failure modes for Experiment 3. At left, the eyetrace intended to capture the cabin instead captured its roof, a much stronger color region. The natural image at right illustrates a problem inherent to color-based object segmentation; the algorithm has no notion that the soldier's white face and gray helmet are both part of the same object. It may be possible to address this issue with a region unification algorithm.

In several cases results illustrated the limitations of object segmentation based on colored regions. For example, we understand the white face of the soldier in Figure 10b and his dark gray helmet to be part of the same object, but as regions of color they are

clearly distinct. One future direction for segmenting complex objects would be the development a "unification" stage that selectively merges previously discovered regions of color within the scope of the eyetrace.

Far more interesting and significant are the results for dataset 2, the real-life retail displays. The median segmentation accuracy for items such as shirts, pants, jackets, and bologna is nearly as high as that for brightly-colored blobs of construction paper on an empty wall. While imperfect (see Figure 11) these numbers suggest that the fusion method is a promising step toward the goal of an eye-driven interface enabling users to "copy and paste" images of environmental objects into electronic storage. Figure 12 shows the prototype succeeding on two trials of the specific motivating problem of enabling AAC users to import images of, and therefore discuss, specific items in a retail setting.

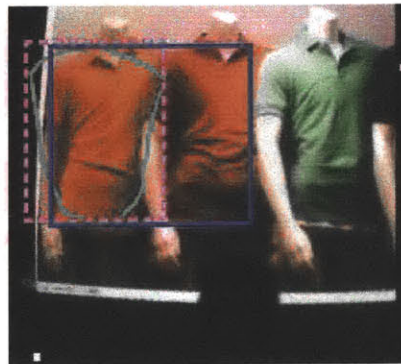


**Figure 11.** Failure mode for Experiment 2. The eyetrace correctly suggests only the pink shirt at left should be in the region of interest. However attracted by the strong color similarity of the red shirt on the right, the fusion algorithm places both shirts in the region of interest. This situation could be prevented by setting a tighter allowable tolerance between the gaze-only solution and the output of the fusion algorithm.

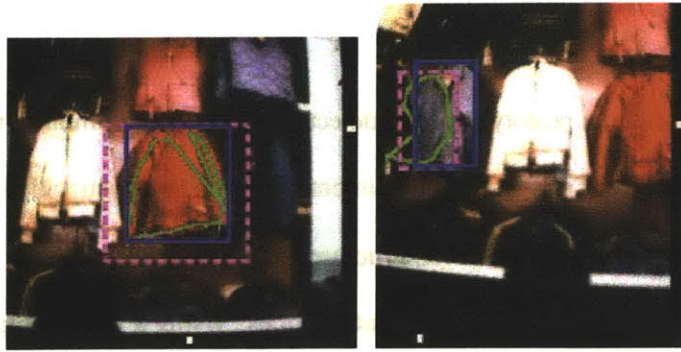


**Figure 12.** Sample segmentation results for Experiment 2. The algorithm successfully discovers the spatial extents of the red and blue jackets.

## Chapter 5: Contributions

We have presented a prototype object detection system that combines top-down information about a user's judgments and intent, derived from eyetracking data, with bottom-up information about the color structure of an image into a single, more robust segmentation result consistent with both data sources. Using a fusion of gaze-based and image-based information, our prototype, Flycatcher, achieved higher object detection accuracy on certain classes of real-world data than approaches based on either signal alone. Related technical contributions of this work are algorithms for processing "eyetraces" of an object into an approximation of the object's bounds and increasing the robustness of image-based hierarchical segmentation through cross-hierarchy agreement.

Flycatcher illustrates the broader idea that unobtrusively leveraging human expertise, e.g., through gaze analysis, can add a great deal of power to human assistive computer systems. This may be particularly true of systems in traditionally difficult areas of image processing.

As an experimental eye-driven interface for high-availability wearable photography Flycatcher also represents a step toward "copy and paste" style visual memory augmentation and the simplified acquisition and communication of ideas in visual form, particularly for the speech disabled. Toward that end we are working to integrate Flycatcher into an experimental assistive communication device under development at Northeastern University[14].



## References

1. Eurotechnology Japan K.K. *Camera phones: Disruptive innovation for imaging (market and trend report, 4<sup>th</sup> version)*, January 14, 2004.
2. Roy, D.K., Ghitza, Y., Bartelma, J., & Kehoe, C. *Visual memory augmentation: Using eye gaze as an attention filter*. Submitted 2004.
3. Gulens, M. (December 2000) *The AAC Mentor Project at Penn State University*. Retrieved July 2004 from <http://mcn.ed.psu.edu/~mentor/Public/aac.html>
4. Ross, M.G. and Kaelbling, L.P. *A systematic approach to learning object segmentation*. NIPS 2003 Workshop on Open Challenges in Cognitive Vision, December 2003.
5. DiMattia, P., Curran, F.X., and Gips, J. *An eye control teaching device for students without language expressive capacity: EagleEyes*. Edwin Mellen Press, 2001.
6. Ware, C. and Mikaelian, H.H. *An evaluation of an eye tracker as a device for computer input*. In J.M. Carroll & P.P. Tanner, eds, CHI + GI 1987 Conference Proceedings, SIGCHI Bulletin, ACM, pp. 183-188. Special issue.
7. *Canon Advantage Eye Controlled Focus*. (n.d.) Retrieved July 2004 from <http://consumer.usa.canon.com/ir/controller?act=CanonAdvantageTopicDtlAct&id=2649>
8. *IBM Almaden Research Center: Creating computers that know how you feel*. (n.d.) Retrieved July 2004 from <http://www.almaden.ibm.com/cs/BlueEyes/index.html>
9. Yarbus, A.L. *Eye Movements and Vision*. Translated by Basil Haigh. Plenum Press: New York, 1967.
10. Martin, D. and Fowlkes, C. (November 12, 2003) *The Berkeley Segmentation Dataset and Benchmark*, retrieved June 2004 from <http://www.cs.berkeley.edu/projects/vision/grouping/segbench/>
11. Forsyth, D.A. and Ponce, J. *Computer Vision: A Modern Approach*. Prentice Hall, 2002.
12. Kropatsch, W.G. and Haxhimusa, Y. *Grouping and Segmentation in a Hierarchy of Graphs*. Proceeding of the 16th IS&T/SPIE Annual Symposium, 2004.
13. Hill, D. *A Vector Clustering Technique*. Mechanised Information Storage, Retrieval and Dissemination, North-Holland, Amsterdam, 1968.
14. Patel, R. and Pilato, S. *A Visually-Oriented, Context-Engaged Language Learning and Communication Aid*.

## **Appendix A: Subject Instructions for Experiments**

In this experiment you will help test an eye-driven interface for designating important regions in a scene. The experiment consists of one set of approximately 20 trials. In each trial, I will show you an image with the overhead projector and briefly describe an area of the picture. Your job is to cut out the area by tracing an outline of the region with your eyes. Press the spacebar once when you begin tracing, and once as you finish.

The trials will be separated by several seconds apiece. Your signal to proceed will be my reading the next description. When you are waiting between trials feel free to look wherever you choose. Throughout, there is no pressure to proceed either very fast or very slow; move your eyes naturally and comfortably.